

Limiting Current Density of Oxygen Reduction under Ultrathin Electrolyte Layers: From the Micrometer Range to Monolayers

Xiankang Zhong,^[a] Matthias Schulz (née Uebel),^[b] Chun-Hung Wu,^[b] Martin Rabe,^[b] Andreas Erbe,^[c] and Michael Rohwerder*^[b]

The oxygen reduction reaction (ORR) under ultrathin electrolyte layers is a key reaction in many processes, from atmospheric corrosion to energy conversion in fuel cells. However, the ORR current under ultrathin electrolyte layers is difficult to measure using conventional electrochemical methods. Hence, reliable data are scarce for the micrometer range and totally missing for the sub-micrometer range of the electrolyte layer thickness. Here, we report a novel hydrogen-permeation-based approach

to measure the ORR current underneath thin and ultrathin electrolyte layers. By using a Kelvin-probe-based measurement of the potential, which results from dynamic equilibrium of oxygen reduction and hydrogen oxidation, and the corresponding hydrogen charging current density, the full current-potential relationship can be constructed. The results shed a new light on the nature of the limiting current density of ORR underneath ultrathin layers of electrolyte.

1. Introduction

From fuel cells to atmospheric corrosion, electrochemical reactions underneath ultrathin electrolyte layers play an important role in quite a number of technically highly relevant processes. In fuel cells or electrolyzers, very high reaction rates of reactive gases, such as, for example, the reduction of oxygen in fuel cells, are the target; whereas, in atmospheric corrosion, high reaction rates are undesired. In the latter, oxygen reduction is often observed to determine the corrosion rates.^[1,2] It is well known that initially with decreasing electrolyte layer thickness the diffusion limited oxygen reduction rate will increase proportionally to the inverse of the thickness.^[1–5] This is also generally assumed to be the reason for the high reaction rates achievable in fuel cells. The reaction interface e.g. in proton exchange membrane fuel cells is the three-phase boundary between the catalyst (and its support), the “liquid”/

polymer phase (water and/or ionomer) and the gaseous phase, i.e. the reactive gas. The direct access of the reactive gas to the catalyst allows very high geometric current densities in the range of a few A/cm².^[6] Such high current densities cannot be provided by rotating disk electrodes (RDE), where the transport of reactive gas to the catalyst is enhanced by the high rotation speeds which lead to a shrinking of the depletion layer and hence to a higher diffusion limited current density.^[7–9]

In aqueous electrolytes such as aqueous H₂SO₄ or HClO₄, the concentration and the diffusion coefficient of oxygen are both quite low. Even at the rotation rate limit of 10000 rpm, the limiting geometric current density for ORR is only about 14 mA/cm².^[10] At such high rotation speeds the diffusion or depletion layer thickness is in the range of a few micrometers.^[11] These restrictions could be overcome by performing a diffusion correction based on the Koutecky-Levich (K-L) equation,^[12] which in principle provides a means for assessing ORR at higher overpotentials where mass transport becomes an issue. Extrapolation of the kinetic current densities to potentials more relevant for fuel cell systems, however, can be extremely inaccurate, because of the possibility of potential-dependent Tafel slopes. In literature, electrolyte-dependent ORR activities are usually assigned to a site blocking mechanism. Hence, a careful data analysis has to be carried out in order to ensure a correct extrapolation, as was recently reported by Zana et al.^[8]

Direct experimental access to such high kinetic current densities as achieved in fuel cells would require thicknesses of the depletion layer in the range of 100 nm or below. This is not achievable for RDE, but shrinking the electrolyte layer thickness is the idea behind the so called floating electrode concept that allows reaching geometric current densities in the A/cm² range,^[13–22] where the catalyst is deposited onto a thin porous substrate that is floating on the electrolyte surface. The reactant gas is provided from above. At the pores the catalyst, electrolyte and the gas phase form three-phase boundaries where fast

[a] Dr. X. Zhong


State Key Laboratory of Oil and
Gas Reservoir Geology and Exploitation
Southwest Petroleum University
Xindu Street 8, Xindu District, Chengdu
Sichuan Province 610500, China


[b] Dr. M. Schulz (née Uebel), Dr. C.-H. Wu, Dr. M. Rabe, PD Dr. M. Rohwerder

Dep. Interface Chemistry and Surface Engineering
Max-Planck-Institut für Eisenforschung GmbH
Max-Planck-Str.1, D-40237 Düsseldorf
E-mail: rohwerder@mpie.de

[c] Prof. Dr. A. Erbe

Dep. Materials Science and Engineering
NTNU, Norwegian University of Science and Technology
NO-7491 Trondheim, Norway

 Supporting information for this article is available on the WWW under <https://doi.org/10.1002/celec.202100083>

 © 2021 The Authors. ChemElectroChem published by Wiley-VCH GmbH. This is an open access article under the terms of the Creative Commons Attribution License, which permits use, distribution and reproduction in any medium, provided the original work is properly cited.

access of protons as well as of oxygen is achieved.^[13,14] Closer to the situation within a fuel cell is the so called gas diffusion electrode approach, where instead of a porous substrate a suitable membrane, such as a Nafion membrane is used, upon which the catalyst layer and gas diffusion layer are placed.^[20,23,24]

However, from atmospheric corrosion it is well known that below about 10–20 μm the mass transport does not increase anymore with further decreasing thickness of the electrolyte layer. This is generally accepted to be due to the oxygen uptake process, i.e. the dissolution of oxygen into the electrolyte becomes rate controlling, leading to maximum current densities for oxygen reduction in the range of a few mA/cm^2 once the thickness gets below about 10 μm .^[1–5] This raises the question how to explain the high current densities observed with floating electrode set-ups, gas diffusion electrode or in fuel cells. Although there the reactions take place at three phase boundaries, i.e., underneath effective electrolyte layers with a thickness well below 10 μm , where indeed fast transport is ensured, an uptake determined limitation should also be expected in these cases.

Until now, no reliable tool or method for measuring ORR current densities under ultrathin electrolyte layers with a thickness below the micrometer range has been reported. Stratmann et al. built an electrochemical set-up based on a Kelvin probe as reference electrode which allows the measurement of polarization curves on metal surfaces which are covered by electrolyte layers as thin as a few micrometers.^[4] Nishikata et al. managed to perform measurements with electrolyte layers down into the 10 μm range by use of a special electrode assembly.^[25] However, studies related to thinner layers have not been reported yet.

Actually, it is extremely difficult to directly and reliably measure the ORR current under such a thin electrolyte layer using a conventional setup that usually includes a reference electrode and a counter electrode, since the ionic path between working electrode and counter electrode gets increasingly interrupted with a decrease of electrolyte layer thickness as a consequence of nearly unavoidable discontinuous distribution of the electrolyte layer between working electrode and counter electrode. Furthermore, large Ohmic drops between the counter and the working electrode cause additional problems.^[25] Hence, the development of an approach which can be used to measure ORR current under ultrathin electrolyte layers would be of great importance.

In our previous work,^[26,27] we developed a hydrogen permeation based potentiometric approach that was successfully used to indirectly measure the ORR current in bulk solution using a conventional reference system. Namely, the current-potential relationship curve of oxygen reduction reaction on an electrode surface can be constructed by measuring the potential resulting from dynamic equilibrium of oxygen reduction and hydrogen oxidation and the corresponding hydrogen charging current density at its backside. This approach was demonstrated to work well for electrodes immersed into bulk electrolytes. However, it was not yet applied for the measurement of ORR currents under ultrathin electrolyte layers.

Here we report now the possibility, to use this hydrogen permeation based potentiometric approach to study ORR under ultrathin electrolyte layers from the micrometer range to monolayers, by applying a Kelvin probe as reference electrode instead of a conventional one. The application of Kelvin probes as reference electrodes is contactless and hence can be used even for measuring potentials underneath ultrathin electrolyte layers, as introduced by Stratmann et al.^[4] and further also discussed by Hausbrand et al.^[28] and Turcu et al.^[29] For the investigation of ORR underneath electrolyte layers in the micrometer range, a thin and spread-out electrolyte droplet on palladium was employed. At the edge of a thin droplet, the electrolyte layer has a low thickness, which due to the high Ohmic resistances in this ultra-low thickness range should enable the measurement of the local ORR rate by measuring the local dynamic steady state potential resulting from ORR and hydrogen oxidation reaction (HOR). This is achieved by using a Scanning Kelvin Probe (SKP) with sufficiently high resolution. Furthermore, current densities of ORR under electrolyte films in the monolayer range will also be reported, obtained by exposing the Pd surface to oxygen containing atmospheres of controlled humidity.

2. Results and Discussion

The developed set-up for the hydrogen permeation based potentiometric approach is schematically illustrated in Figure 1 where the top (entry) side of sample is used for hydrogen charging and the bottom (exit) side is for the measurement of the equilibrium potential of hydrogen oxidation and oxygen reduction underneath ultrathin electrolyte layers by Scanning Kelvin Probe. The experimental details can be found in the Supporting Information.

Figure 2 shows the thickness of the electrolyte layer at different distances from the edge of a droplet of aqueous saturated NaCl, the potentials obtained by SKP measured on its surface and the corresponding current densities applied at the entry side. The current density vs. potential curves deduced from the hydrogen charging current density at the entry side and the equilibrium potential at the exit side under the droplet are shown in Figure 3. For all thicknesses, clearly two successive current density plateaus can be seen: one plateau with the current density around $-12 \mu\text{A}/\text{cm}^2$, and another one with the current density about $-24 \mu\text{A}/\text{cm}^2$, as marked in Figure 3.

The observation of two plateaus, with the limiting current density of the second plateau being about twice of the one of the first plateau, indicates that for these experiments at lower overpotentials a two-electron pathway and at higher overpotentials a four-electron pathway prevail for the oxygen reduction on Pd.^[30–34] Such observations are common and are observed on a number of electrode materials and at different pH, see literature.^[30–37] This is often explained by Yeager's theory of the 2-electron pathway reduction to peroxide and the 4-electron pathway reduction to water.^[38] However, for instance for catalysts in fuel cells only the four-electron pathway is desirable, as it is the case e.g. on Pt catalysts, for which recent

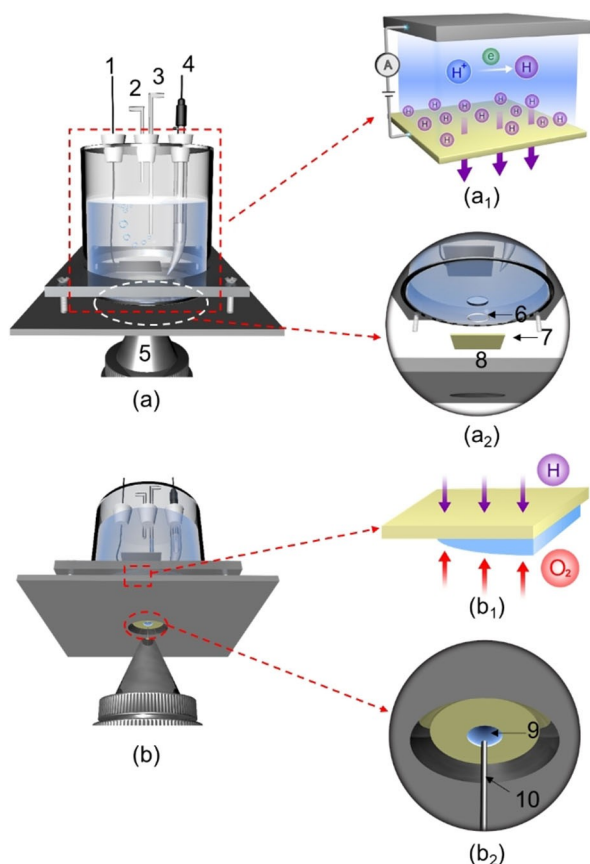


Figure 1. Schematic diagram of the experimental setup a) front view: the upper side is the hydrogen charging cell, as simply illustrated in (a₁), in which H⁺ is electrochemically reduced to atomic H that can permeate through the Pd membrane and finally reaches the exit side where it can react with O₂. a₂) The enlarged view between hydrogen charging cell and exit side of hydrogen. b) Lateral view: b₁) the permeating H and the O₂ uptake, and b₂) enlarged view of the H exit side and the droplet. A droplet is hanging down from the exit side surface. The number in the figure indicates: 1 – Counter electrode, 2 – Ar gas outlet, 3 – Ar gas inlet, 4 – Reference electrode, 5 – SKP head, 6 – O ring, 7 – Pd membrane, 8 – Sample holder, 9 – Droplet and 10 – SKP-tip.

works based on DFT suggest indeed a direct four electron pathway.^[39,40] The focus here is, however, on the limiting current densities. It should be noted that the second plateau of limiting current is incomplete because the potential is pinned as the current density increases due to the formation of palladium hydride (β -Pd-H), resulting in the constructed current density vs. potential curves to show a sudden apparent step increase of cathodic current densities,^[26] see shaded data in Figure 3.

The obtained limiting current densities do not show significant differences for electrolyte thicknesses in the range between about 0.1 μm and 24 μm . It should be noted that the height resolution of the SKP at the edge of the droplet is about 100 nm, i.e. “0 μm ” in Figure 3 indicates a thickness range around or below 100 nm. The current density vs. potential curves shift towards higher potentials with decreasing electrolyte thickness, especially when the thickness gets below the 10 μm range. This is not understood yet.

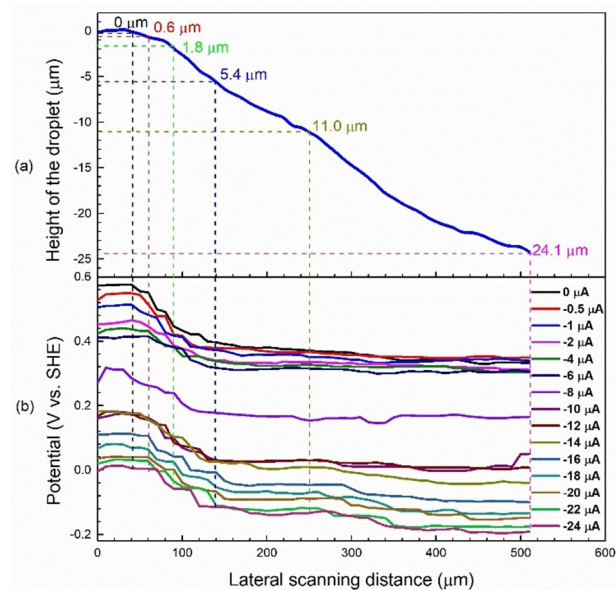


Figure 2. a) Height profile of the droplet (saturated NaCl) from the edge (left side) toward the center (right side), measured by SKP. “0 μm ” indicates a thickness range around or below 100 nm since the height resolution of the SKP at the edge of the droplet is about 100 nm. b) Potential distribution of the sample surface from the vicinity to the center direction of the droplet. The thickness of electrolyte layer at each point on the sample surface along the X-axis can be deduced from this height profile curve.

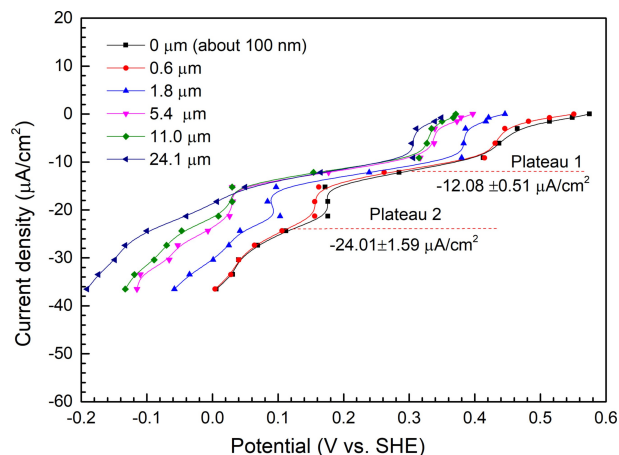


Figure 3. Current density vs. potential curves deduced from hydrogen charging current at the entry side and equilibrium potential at the exit side under a droplet. The electrolyte thicknesses are marked in Figure 2 with dashed lines. Spline is used to connect the data for each thickness. The red dotted lines indicate the current densities at the two current plateaus. The shaded data do not show the correct current density-potential correlation as the formation of palladium hydride pins the potential as the current densities increase.

To verify the validity of the results obtained from the hydrogen permeation based potentiometric approach, another experiment was conducted using a more conventional three-electrode set-up but with the reference electrode replaced by an SKP (similar to Stratmann et al.^[41]) under the same test conditions. Electrolyte layers with thicknesses of 26, 70 and

4030 μm were prepared (the experimental details can be found in the Supporting Information).

The results obtained by using this more conventional set-up are shown in Figure 4. It can be seen that the limiting current density for oxygen reduction increases with the decreasing thickness of electrolyte layer, see the marked current density data (Figure 4a). This is in good agreement with the results obtained by Stratmann et al.^[4] and Nishikata et al.^[5] Figure 4b shows the comparison of results obtained from both approaches, in which the thickness of the electrolyte layer is very close for both experiments. The 26 μm are at the lower limit of the thickness that we could reach with the more conventional set-up. It is found that the limiting current regions for oxygen reduction match very well (Figure 4b). Therefore, it can be considered that the hydrogen permeation based potentiometric approach is reliable to be used to measure ORR current densities in ultrathin electrolyte layers.

Figures 3 and 4 show that the limiting current densities within the 2-electron potential range are relatively similar for electrolyte layer thicknesses below a few micrometers. For the second plateau at more negative potentials this correlation is more difficult to see, because of the formation of palladium hydride ($\beta\text{-Pd-H}$) as mentioned above. This observed independ-

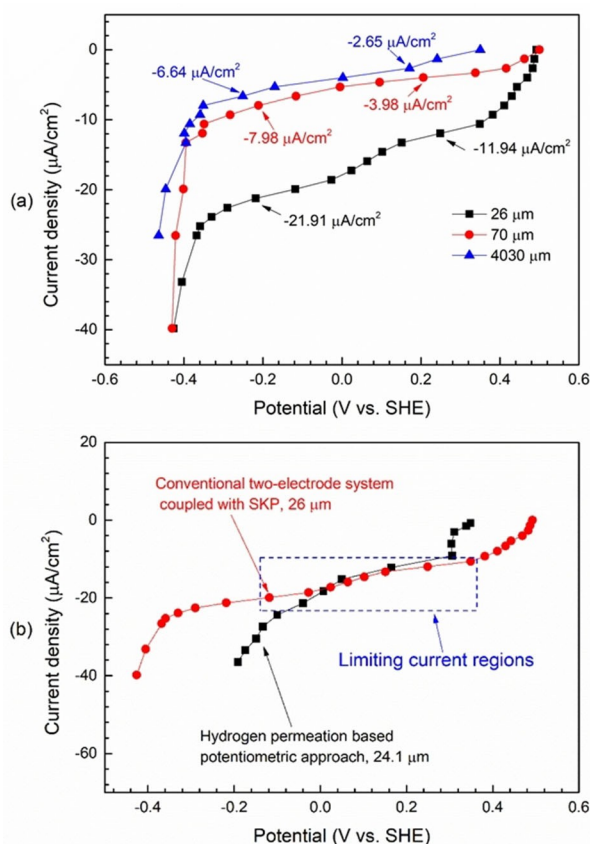


Figure 4. a) The current density vs. potential curves obtained from conventional two-electrode system and SKP as a reference electrode. The marked current densities are used to indicate the two different current densities plateaus and b) the comparison of current density vs. potential curves obtained hydrogen permeation based potentiometric approach and conventional two-electrode system coupled with SKP.

ence of the limiting current density is in good agreement with earlier reports that the oxygen uptake at the surface of the electrolyte becomes rate determining once the thickness of the electrolyte layer gets into the range of a few tens of micrometers and hence the current density is limited to a constant value, even down to the range of a few micrometers.^[4,5]

Our results show that limiting current does not change even when the thickness of the electrolyte layer goes well below the micrometer range down to about 100 nm. No tendency for a change in uptake kinetics can be observed, as can be seen directly from the nearly identical current density vs. potential curves for about 0.6 μm electrolyte thickness and the one of the about 100 nm thick electrolyte layer. This means that even an electrolyte layer of only about 100 nm thickness would not allow to achieve current densities for oxygen reduction of more than about 2.5 mA/cm^2 (note that our results were obtained at a partial pressure of 10 mbar oxygen, i.e. in order to compare with 1 bar of oxygen atmosphere our current densities have to be multiplied by 100, see Figure 3).

However, how is it then possible that e.g. by use of floating electrodes orders of magnitude higher current densities are reported,^[14] while here the uptake limitation is found even for very thin electrolyte layers of down to 100 nm?

It is not surprising that even for ~ 100 nm electrolyte thickness the uptake kinetics at the surface of the electrolyte is the same as for an electrolyte layer of several micrometers or even thicker, as the molecular structure is not expected to differ much. However, this will change once the thickness of the electrolyte layer gets even much thinner, into the range of a few tens of nanometers or even below.

Experiments on such thin electrolyte layers are difficult to perform, even with the approach presented here, because it is difficult to control the thickness of the electrolyte layer in this range. Hence, another approach was taken. The electrolyte layer on a surface can be defined in the monolayer range just by adjusting the humidity in the environment of that surface, see ellipsometry data in Supporting Information (Figure S2). In Figure 5, constructed Tafel plots derived from measurements performed at 93% relative humidity (rh), at which about a monolayer of electrolyte is formed, are shown (Figure S2). As can be seen from the Tafel plots, there is no limiting current density. A Tafel slope of about 60 mV/decade at low current densities is found, for the higher current densities 120 mV/decade, as is also reported for ORR on Pd in bulk electrolytes.^[41] For the lower oxygen partial pressures only the high current density range was measured since low current densities are prone to artefacts from contamination. As can be seen, the current density at a given potential increases proportionally with the oxygen partial pressure, again as also found for Pd immersed in bulk electrolyte.^[41] For 1% oxygen content current densities of up to 400 $\mu\text{A}/\text{cm}^2$ were measured, which is hence equivalent to up to 40 mA/cm^2 for humid oxygen at 1 bar O_2 (to measure this directly for humid oxygen of 1 bar is not feasible, as such high hydrogen charging from the backside was not achievable; hence, the use of 10 mbar oxygen). This means that for such monolayers there is no uptake limitation for oxygen.

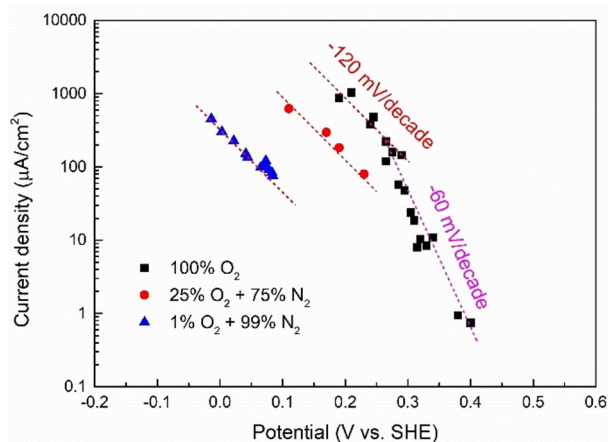


Figure 5. Current-potential correlation obtained on a polycrystalline palladium sample exposed to different O_2 partial pressures environment at 93 % r.h. Into the measured data straight lines indicating a Tafel slope of 60 mV/decade at lower current densities and of 120 mV/decade at higher current densities are drawn as dashed lines.

It is hypothesized that this increased accessibility of O_2 for the case of monolayer covered metal is caused by a difference in the structural dynamics of water at the water film / gas interface. It is well established for a series of metals, semiconductors and insulators, both in simulation and vibrational spectroscopic experiment^[42–46] that strongly bound interfacial water has a different coordination of the water molecule compared to bulk water. Differences in water structure at the surface were also found for solvated Pd.^[46] IR spectra of the OH stretching modes e.g. in porous silica with different pore sizes shows deviations from the bulk water spectrum up to 30 nm pore diameter, indicating a long range coupling between water molecules.^[47] Such long range coupling in bulk water is also suggested by simulations and 2D IR experiments.^[48–50] The exact water thickness value for the transition is beyond the scope of the current work.

Our results strongly indicate that high current densities achieved with a floating electrode or a diffusion cell approach originate from the outermost perimeter of the three-phase boundary zone, where the electrolyte layer is at most a few nanometers thick.

3. Conclusions

In this study, the ORR current under ultrathin aqueous electrolyte layers from the micrometer range to monolayers was successfully measured, using a hydrogen permeation based potentiometric approach utilizing a Kelvin probe as reference electrode. Through this approach, reliable current-potential curves of ORR under ultrathin electrolyte layers can be constructed by measuring the dynamic equilibrium potential of oxygen reduction and hydrogen oxidation on the surface, and the corresponding hydrogen charging current density at the backside of the sample.

Under electrolyte layers of aqueous saturated NaCl in the thickness range between 24 μm and 0.1 μm , the limiting current densities do not show significant differences. At 1 bar oxygen partial pressure, the current densities in this thickness range are limited to about 2.5 mA/cm^2 due to oxygen uptake limitation at the surface of the electrolyte film. This value for the limiting current density due to oxygen uptake limitation is in good agreement with values reported in the literature, if the dependence of oxygen solubility on electrolyte concentration is also taken into account (see Stratmann et al.^[4]). While the investigations discussed here were carried out on aqueous saturated NaCl electrolyte layers, uptake limitation has been, however, also reported for chloride, perchlorate and sulphate containing electrolytes of different concentrations and pH.^[4,5,25] Hence, we are sure that our observations are not restricted to aqueous saturated NaCl electrolyte and this limitation will also exist in the case of other aqueous electrolyte compositions and thicknesses down to the range of at least several tens of nanometers, if not down to even just several nanometers. This rate limitation breaks down for ultrathin electrolyte layers in the monolayer range, enabling ORR current densities in the A/cm^2 range. Obviously, the molecular structure of the electrolyte in the outermost periphery of the three-phase boundary plays a crucial role. Further research on this should provide new important insights.

While oxygen uptake limitation is in principle well known in corrosion science, in other fields of electrochemistry it is usually not much discussed. For instance, in order to reach the targeted high current densities as they occur in membrane electrode assemblies (MEAs), different experimental approaches beyond high speed rotating disk, are utilized, such as floating electrodes and gas diffusion electrodes.^[13–22] The idea in these approaches is that electrolyte just wets the catalyst layer so that the reactant gas does not have to diffuse through bulk electrolyte and thus diffusion limitation will be significantly reduced. However, our results show that even for very thin electrolyte layers wetting the surface, oxygen uptake limitation should prevent the targeted high current densities unless they are in the monolayer range or at most a few nanometers thick. Only underneath such ultrathin layers ORR can reach the targeted current densities. In floating electrode or diffusion electrode experiments this are the regions at the outermost periphery of the three-phase boundary region of aqueous electrolyte, support/catalyst and gas phase.

Although recent simulation work on ORR at catalysts in gas diffusion electrodes provides high current densities, being in good agreement with experimental results, even when assuming continuous thin electrolyte films in the range of 25–300 nm covering the catalyst particles and without considering uptake control,^[51] this does not contradict the results reported here. In fact, for the same kind of electrode it was reported that the gas-liquid interface is by far more complex than a homogeneously thin film, rather being characterized by a high density of microdroplets, as was revealed by operando X-Ray imaging.^[52] Hence, it is proposed here that also in that case the main O_2 uptake is occurring exactly in the ultrathin boundary regions of these droplets.

Most likely also regions which are not in direct contact with the three-phase boundary region but which are also not too far away and connected to the electrolyte layer by the ionomer networks, which in a MEA are providing the proton transport, are playing a crucial role. The oxygen uptake at the surface of ionomer layers is also known to show a limitation, but it is by far not as severe as it is at the surface of aqueous electrolyte.^[53] Thin water layers are by far more critical, as they result in nearly three orders of magnitude lower oxygen uptake rates. Nevertheless, the development of ionomers which are more permeable for oxygen and also have improved oxygen uptake is still an important topic of current research.^[54]

Maybe the most fascinating result of this work is that the electrochemical oxygen reduction reaction on the surface of palladium just covered by one to two monolayers of water, is in principle the same as on an electrode immersed in acidic bulk electrolyte, just without the mass transport limitation for oxygen. Because for an electrode immersed in electrolyte the double layer is more extended, this directly raises questions about the structure of the electrochemical double layer, which is here confined to just one or two monolayers with protons as counter ions, and how this determines the reaction kinetics. Further research in our group will concentrate on this object. From a more practical perspective, this indicates that “bare” catalyst particles, which are just covered by adsorbed water in the monolayer range, can be electrochemically active and can provide ORR at high rates. For ORR on a “bare” catalyst particle in a MEA, protons have to be delivered from the ionomer in the vicinity. It is reported that proton transport can readily occur on the surface of the metallic catalyst, e.g. for Pt via Pt-OH or Pt-H.^[55–57] Thus, as supported by our results, catalysts not covered by ionomer may play an important role in the overall ORR activity of the MEA. This is in agreement with recent works where it is reported that catalyst particles located in small pores inside porous carbon and which are thus close to but not in direct contact with ionomer, show high electrochemical activity for ORR at high current densities,^[57] compared to catalyst covered by ionomer where the interaction with the ionomer is observed to result in decreased catalytic activity.^[54] Although it is suggested by some authors^[58] that a direct correlation of the 3D ionomer layer structure to the electrochemical response of the electrode can be made, our results show that the distribution of the “bare” catalyst particles at least in the vicinity of the ionomer also have to be taken into account.

Hence, our findings provide new insights concerning the origin of the high current densities achieved for ORR in fuel cells, diffusion electrode or floating electrode experiments and shed new light on the nature of the three-phase boundary zone.

Furthermore, the results reported here should be of importance for obtaining a better understanding also of atmospheric corrosion. For instance, besides the cathodic activity in micro-droplets that are forming around the larger primary droplets,^[59] it might be also important to consider the activity in the seemingly inactive area between them, which is just covered by ultrathin electrolyte layers in the monolayer range.

Finally, we point out that the approach presented here may find application also for studies on other electrode materials and of other cathodic reactions than palladium and oxygen reduction. The method just requires that a hydrogen loading from the backside of the sample is possible and that hydrogen permeation to the surface is not blocked. This could be achieved in a first step with thin layers of the materials of interest to be deposited onto a Pd membrane. If the layers are thin enough, then even for materials with low H permeation high enough hydrogen permeation rates can be achieved. But even more challenging applications seem possible. For instance, individual nanoscopic particles of catalyst could be deposited on a Pd membrane and laterally resolved studies could be carried out by using an AFM based Kelvin probe approach (Scanning Kelvin Probe Microscopy, SKPFM). However, this will require intense further research. In fact, there are a number of possible applications thinkable, many of which are not addressable by other approaches. But it has to be pointed out, that this is not a standard technique that can be easily and directly applied on different systems. It is rather an experimental tool that needs to be adjusted to the system to be addressed.

Acknowledgements

This work was funded by the Max Planck Society and the Deutsche Forschungsgemeinschaft (DFG, German Research Foundation) under Germany's Excellence Strategy - EXC 2033 - 390677874 - RESOLV. The author (X. Z.) was also supported by the Alexander von Humboldt-Stiftung (www.humboldt-foundation.de). Open access funding enabled and organized by Projekt DEAL.

Conflict of Interest

The authors declare no conflict of interest.

Keywords: fuel cell · electrochemistry · oxygen reduction reaction · ultrathin electrolyte layer · hydrogen permeation

- [1] M. Ito, A. Ooi, E. Tada, A. Nishikata, *J. Electrochem. Soc.* **2020**, *167*, 101508.
- [2] H. Simillion, O. Dolgikh, H. Terryn, J. Deconinck, *Corros. Rev.* **2014**, *32*, 73–100.
- [3] H. Simillion, N. Van den Steen, H. Terryn, J. Deconinck, *Electrochim. Acta* **2016**, *209*, 149–158.
- [4] M. Stratmann, H. Streckel, K. T. Kim, S. Crockett, *Corros. Sci.* **1990**, *30*, 715–734.
- [5] A. Nishikata, Y. Ichihara, Y. Hayashi, T. Tsuru, *J. Electrochem. Soc.* **1990**, *144*, 1244–1252.
- [6] H. A. Gasteiger, S. S. Kocha, B. Sompalli, F. T. Wagner, *Appl. Catal. B* **2005**, *56*, 9–35.
- [7] W. Chen, L. W. Liao, J. Cai, Y.-X. Chen, U. Stimming, *J. Phys. Chem. C* **2019**, *123*, 29630–29637.
- [8] A. Zana, G. K. H. Wiberg, Y. J. Deng, T. Ostergaard, J. Rossmeisl, A. Arenz, *ACS Appl. Mater. Interfaces* **2017**, *9*, 37176–38180.
- [9] A. J. Martin, A. M. Chaparro, M. A. Folgado, J. Rubio, L. Dazaa, *Electrochim. Acta* **2009**, *54*, 2209–2217.
- [10] A. R. Kucernak, E. Toyoda, *Electrochem. Commun.* **2008**, *10*, 1728–1731.

- [11] C. E. Banks, A. O. Simm, R. Bowler, K. Dawes, R. G. Compton, *Anal. Chem.* **2005**, *77*, 1928–1930.
- [12] F. J. Vidal-Iglesias, J. Solla-Gullón, V. Montiel, A. Aldaz, *Electrochem. Commun.* **2012**, *15*, 42–45.
- [13] C. M. Zalitis, D. Kramer, A. R. Kucernak, *Phys. Chem. Chem. Phys.* **2013**, *15*, 4329–4340.
- [14] C. Zalitis, A. Kucernak, X. Lin, J. Sharman, *ACS Catal.* **2020**, *10*, 4361–4376.
- [15] S. Martens, L. Asena, G. Ercolano, F. Dionigi, C. Zalitis, A. Hawkins, A. M. Bonastre, L. Seidl, A. C. Knoll, J. Sharman, P. Strasser, D. Jones, O. Schneider, *J. Power Sources* **2018**, *392*, 274–284.
- [16] G. W. Sievers, A. W. Jensen, V. Brüser, M. Arenz, M. Escudero-Escribano, *Surfaces* **2019**, *2*, 336–348.
- [17] Y. Hu, Y. Jiang, J. O. Jensen, L. N. Cleemann, Q. Li, *J. Power Sources* **2018**, *375*, 77–81.
- [18] G. K. H. Wiberg, M. Fleige, M. Arenz, *Rev. Sci. Instrum.* **2015**, *86*, 024102.
- [19] B. A. Pinaud, A. Bonakdarpour, L. Daniel, J. Sharman, D. P. Wilkinson, *J. Electrochem. Soc.* **2017**, *164*, F321–F327.
- [20] M. Inaba, A. W. Jensen, G. W. Sievers, M. Escudero-Escribano, A. Zana, M. Arenz, *Energy Environ. Sci.* **2018**, *11*, 988–994.
- [21] L. Pan, S. Ott, F. Dionigi, P. Strasser, *Curr. Opin. Electrochem.* **2019**, *18*, 61–71.
- [22] Z. Ma, Z. P. Cano, A. Yu, Z. Chen, G. Jiang, X. Fu, L. Yang, T. Wu, Z. Bai, J. Lu, *Angew. Chem. Int. Ed.* **2020**, *59*, 18334–18348.
- [23] G. K. H. Wiberg, M. J. Fleige, M. Arenz, *Rev. Sci. Instrum.* **2014**, *85*, 085105.
- [24] G. W. Sievers, A. W. Jensen, J. Quinson, A. Zana, F. Bizzotto, M. Oezaslan, A. Dworzak, J. J. K. Kirkensgaard, T. E. L. Smitshuysen, S. Kadkhodazadeh, M. Juelsholt, K. M. Ø. Jensen, K. Anklam, H. Wen, J. Schäfer, K. Čépe, M. Escudero-Escribano, J. Rossmeisl, A. Quade, V. Brüser, M. Arenz, *Nat. Mater.* **2020**.
- [25] A. Nishikata, Y. Ichihara, T. Tsuru, *Corros. Sci.* **1995**, *37*, 897–911.
- [26] D. Vijayshankar, T. H. Tran, A. Bashir, S. Evers, M. Rohwerder, *Electrochim. Acta* **2016**, *189*, 111–117.
- [27] D. Vijayshankar, A. Altin, C. Merola, A. Bashir, E. Heinen, M. Rohwerder, *J. Electrochem. Soc.* **2016**, *163*, C778–C783.
- [28] R. Hausbrand, M. Stratmann, M. Rohwerder, *J. Electrochem. Soc.* **2008**, *155*, C369–C379.
- [29] F. Turcu, M. Rohwerder, *Electrochim. Acta* **2007**, *53*, 290–299.
- [30] N. M. Marković, H. A. Gasteiger, P. N. Ross, *J. Phys. Chem.* **1995**, *99*, 3411–3415.
- [31] B. Li, J. Prakash, *Electrochem. Commun.* **2009**, *11*, 1162–1165.
- [32] B. B. Blizanac, P. N. Ross, N. M. Markovic, *Electrochim. Acta* **2007**, *52*, 2264–2271.
- [33] Y. Lin, X. Cui, X. Ye, *Electrochem. Commun.* **2005**, *7*, 267–274.
- [34] R. G. Morais, N. Rey-Raap, J. L. Figueiredo, M. F. R. Pereira, *Beilstein J. Nanotechnol.* **2019**, *10*, 1089–1102.
- [35] M. Zhang, Y. Yan, K. Gong, L. Mao, Z. Guo, Y. Chen, *Langmuir* **2004**, *20*, 8781–8785.
- [36] V. B. Baez, D. Pletcher, *J. Electroanal. Chem.* **1995**, *382*, 59–64.
- [37] Q. Chang, P. Zhang, A. H. B. Mostaghimi, X. Zhao, S. R. Denny, J. H. Lee, H. Gao, Y. Zhang, H. L. Xin, S. Siahrostami, J. G. Chen, Z. C. Chen, *Nat. Commun.* **2020**, *11*, 2178.
- [38] E. Yeager, *J. Mol. Catal.* **1986**, *38*, 5–25.
- [39] K. Holst-Olesen, L. Silvioli, J. Rossmeisl, M. Arenz, *ACS Catal.* **2019**, *9*, 3082–3089.
- [40] V. Tripković, E. Skúlason, S. Siahrostami, J. K. Nørskov, J. Rossmeisl, *Electrochim. Acta* **2010**, *55*, 7975–7981.
- [41] D. B. Sepa, M. V. Vojnovic, L. M. Vracar, *Electrochim. Acta* **1987**, *32*, 129–134.
- [42] D. B. Asay, A. L. Barnette, S. H. Kim, *J. Phys. Chem. C* **2009**, *113*, 2128–2133.
- [43] D. B. Asay, S. H. Kim, *J. Phys. Chem. B* **2005**, *109*, 16760–16763.
- [44] B. A. Gawel, A. Ulvesoen, K. Lukaszuk, B. Arstad, A. M. F. Mugggerud, A. Erbe, *RSC Adv.* **2020**, *10*, 29018–29030.
- [45] M. P. Gaigeot, M. Sprik, M. Sulpizi, *J. Phys. Condens. Matter.* **2012**, *24*, 124106.
- [46] S. Beyhan, J. M. Leger, F. Kadirgan, *Appl. Surf. Sci.* **2014**, *321*, 426–431.
- [47] J. Abe, N. Hirano, N. Tsuchiya, *J. Mater. Sci.* **2012**, *47*, 7971–7977.
- [48] B. M. Auer, J. L. Skinner, *J. Chem. Phys.* **2008**, *128*, 224511.
- [49] M. Thämer, L. De Marco, K. Ramasesha, A. Mandal, A. Tokmakoff, *Science* **2015**, *350*, 78–82.
- [50] D. C. Elton, M. Fernandez-Serra, *Nat. Commun.* **2016**, *7*, 10193.
- [51] M. Röhe, A. Botz, D. Franzen, F. Kubanek, B. Ellendorff, D. Öhl, W. Schuhmann, T. Turek, U. Krewer, *ChemElectroChem* **2019**, *6*, 5671–5681.
- [52] M. C. Paulisch, M. Gebhard, D. Franzen, A. Hilger, M. Osenberg, N. Kardjilov, B. Ellendorff, T. Turek, C. Roth, I. Manke, *Materials* **2019**, *12*, 2686.
- [53] T. Suzuki, K. Kudo, Y. Morimoto, *J. Power Sources* **2013**, *222*, 379–389.
- [54] A. Kongkanand, M. F. Mathias, *J. Phys. Chem. Lett.* **2016**, *7*, 1127–1137.
- [55] M. K. Debe, *J. Electrochem. Soc.* **2013**, *160*, F522–F534.
- [56] J. McBreen, *J. Electrochem. Soc.* **1985**, *132*, 1112–1116.
- [57] J. Liu, I. V. Zenyuk, *Curr. Opin. Electrochem.* **2018**, *12*, 202–208.
- [58] M. Lopez-Haro, L. Guétaz, T. Printemps, A. Morin, S. Escibano, P.-H. Jouneau, P. Bayle-Guillemaud, F. Chandezon, G. Gebel, *Nat. Commun.* **2014**, *5*, 5229.
- [59] T. Tsuru, K. I. Tamiya, A. Nishikata, *Electrochim. Acta* **2004**, *49*, 2709–2715.

Manuscript received: January 20, 2021
Accepted manuscript online: February 3, 2021